Wireless Non-contact EEG/ECG Electrodes for Body Sensor Networks

Yu M. Chi and Gert Cauwenberghs
University of California, San Diego
La Jolla, CA 92093

***Abstract*—A wireless EEG/ECG system using non-contact sensors is presented. The system consists of a set of simple capacitive electrodes manufactured on a standard printed circuit board that can operate through fabric or other insulation. Each electrode provides 46dB of gain over a .7-100Hz bandwidth with a noise level of 3.8μV RMS for high quality brain and cardiac recordings. Signals are digitized directly on top of the electrode and transmitted in a digital serial daisy chain, minimizing the number of wires required on the body. A small wireless base unit transmits EEG/ECG telemetry to a computer for storage and processing.**

***Index Terms*—ECG, EEG, Body Sensor, Capacitive Sensing, Non-contact Electrode**

I. Introduction

Body sensor networks will be a key driving force for the wireless health revolution by allowing patients access to their physiological state at anytime in their daily life. Brain and cardiac biopotential signals in the form of EEG and ECG are two critical health indicators that are directly suited for long-term monitoring using body sensor networks. Yet despite advancements in wireless technology and electronics miniaturization, the use EEG/ECG has still been largely limited by the inconvenience and discomfort of conventional wet contact electrodes.

For home use, clinical grade adhesive electrodes are often cited as irritating and uncomfortable leading to low usage compliance. As an alternative, dry electrodes [1] [2] have started becoming much more common-place. However, like wet electrodes, dry electrodes still require direct electrical contact to the skin. In addition, dry electrodes, which do not have the benefit of a conductive gel, are much more sensitive to the condition of the skin and are highly susceptible to motion artifacts. An easier to use and less obtrusive technology is called for to match the advancements made in wireless body sensor networks.

In contrast to wet and dry contact sensors, non-contact capacitive electrodes do not require an ohmic connection to the body. For body sensor applications, this offers numerous advantages since non-contact electrodes require zero preparation, are completely insensitive to skin conditions and can be embedded within comfortable layers of fabric. While the concept of non-contact biopotential sensors is not new, with the first working device reported decades ago [3], a practical device for patient use has yet to be realized. More recently, several authors have presented results from designs utilizing the latest in commercially available discrete low noise amplifiers [4] [5] [6], including some wireless designs [7]. In all cases, the challenges in non-contact sensing have lead to many clever, and often-times, proprietary circuit designs in an effort stabilize the electrode's input.

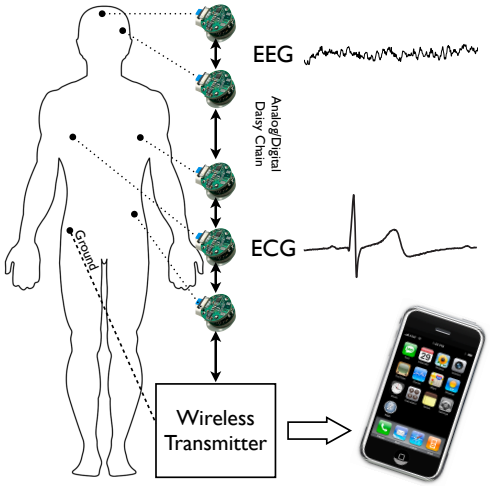

Fig. 1. Block diagram of wireless BSN. The system contains a suite of non-contact EEG and ECG electrodes connected along a single daisy chain that carries the analog and digital signals. A wireless base unit transmits the physiological data to a remote device.

In this paper, we expand on the work previously presented in [8] and [9] by building a sensor with much improved noise performance. In addition, the full design and schematics for a wireless, non-contact EEG/ECG system with features designed for specifically for practical body sensor networks is described.

II. System Design

A high level diagram of the wireless non-contact EEG/ECG system is depicted in Fig. 1. The system contains a set of non-contact biopotential electrodes connected along a single common wire. The sensors can be either in direct contact with the skin or embedded within fabric and clothing. A small base unit powers the entire system and contains a wireless transmitter to send data to a computer or other external device. Near the base unit, a single adhesive or dry contact sensor placed anywhere convenient is used to establish the ground reference for the system.

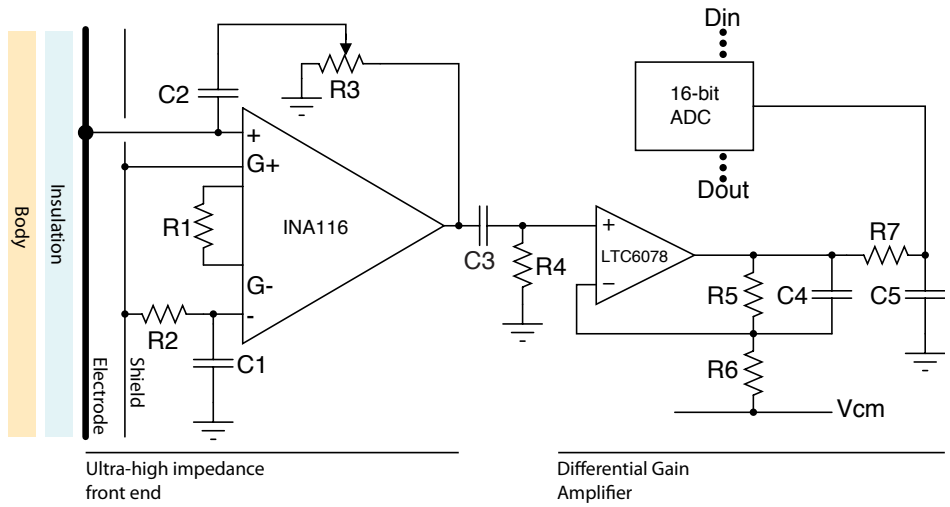

Fig. 2. Full schematic of non-contact electrode showing the ultra-high input impedance front-end, differential amplifier and 16-bit ADC. The nodes Din, Dout and Vcm are carried along the daisy chain.

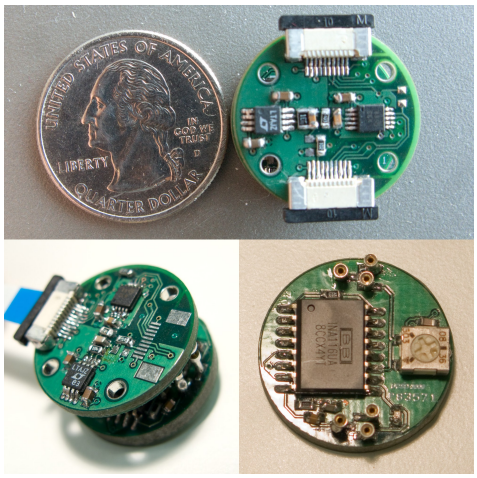

Fig. 3. Picture of the non-contact electrodes. (Top) The upper PCB which contains a differential amplifier and ADC along with the two serial daisy chain connectors. (Bottom Left) A side view of the electrode showing the upper and lower PCBs joined together. (Bottom Right) The lower PCB which contains the ultra-high input impedance amplifier front-end. The bottom of this PCB is a solid, insulated copper fill which functions as the capacitive electrode.

A. Electrode Construction

Each electrode is constructed from two, US quarter sized, PCBs. The upper PCB contains a low noise differential amplifier and a 16-bit ADC. Rather than outputting a single analog signal, the electrode outputs the digitized value, which can be carried in serial daisy chain to drastically reduce the number of wires needed. A miniature 10-wire ribbon cable carries the power supply, digital control as well as analog common mode reference from electrode-to-electrode.

The lower PCB contains the INA116 configured as an ultra-high input impedance amplifier. The bottom surface of the PCB is a solid copper fill, insulated by soldermask, that functions as the electrode. This surface forms a coupling capacitor with the body. An active shield formed by in a solid inner plane protects the electrode from external noise pick-up. To minimize the shield capacitance, an extra thick PCB is used for the electrode. The full schematic of the two PCBs of the non-contact electrode is shown in Fig. 2.

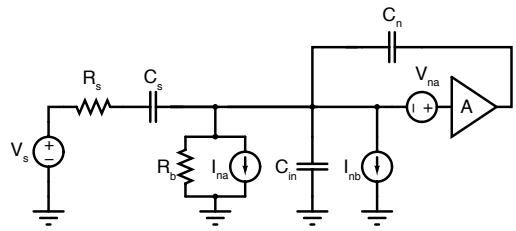

Fig. 4. Circuit model of an amplifier for capacitive sources.

B. Front End Amplifier

Designing an ultra-high input impedance amplifier with low noise levels is the main challenge in implementing non-contact electrodes. Figure 4 depicts a simplified, generic model for a capacitive sensor that is directly applicable to the circuit used in this design. Signal sources from the body (EEG/ECG) can be thought of as a voltage source, V_s, connected to the input of an amplifier via a small coupling capacitance, C_s. All real amplifiers will also have some finite resistance, R_b, and input capacitance. A small amount of positive feedback can be applied through, C_n, to neutralize the effect of the input capacitance for better channel matching and CMRR.

Important noise sources include the input referred voltage noise of the amplifier, V_{na}, the input current noise, I_{na} and the additional current noise, I_{nb}, due to the leakage and conductance of the biasing element. The current noise contribution will either $4kTR$ thermal noise for a resistive device or $2qI$ shot noise for a PN junction. Bootstrapping can be used to electronically boost the effective impedance of the biasing element, but the noise contribution depends only

on the physical resistance or leakage current, illustrating the challenge in finding suitable components for a non-contact sensor. The total input referred noise of a capacitive amplifier can be written as,

$$v_n^2 = v_{na}^2(1 + \frac{C_{in} + C_n}{C_s})^2 + \frac{i_{na}^2 + i_{nb}^2}{\omega^2 C_s^2}, \quad (1)$$

This equation clearly shows the effect of the parasitic input capacitances and leakage currents on the noise performance of the amplifier and the difficulty in designing a non-contact electrode. Any excess input capacitance will directly multiply the effect of the amplifier's input voltage noise as $C_{in} + C_n > C_s$. Furthermore, since biopotential signals are at low frequencies (.1-100Hz), even small amounts of current noise become integrated into large amounts of input voltage noise. This necessitates an an amplifier with both very low input and guard capacitance as well as almost zero leakage currents.

The INA116 by Burr-Brown is an amplifier that is well-known for ultra-high input impedance applications by virtue of its extremely low current noise ($.1fA/\sqrt{Hz}$). However, any circuit introduced to bias the inputs will significantly degrade the noise performance of the amplifier. An extremely difficult to obtain resistor of greater than $1T\Omega$ would be required to match the current noise specification of the INA116. Fortunately, it was found during experiments that the INA116 would reliably charge a floating input to a point inside the allowable input range shortly after power-up purely through leakage currents, removing the need for any external bias network. To remove drift and DC offsets, a low-passed version of the input signal was taken from the non-inverting input's guard and connected to the inverting input. This effectively performs AC coupling without degrading the input impedance and centers the output to mid-rail for maximum signal swing. The overall gain of the first stage can be written as,

$$A_v = (1 + \frac{50k\Omega}{R_1}) \times \frac{sR_2C_1}{1 + sR_2C_1}. \quad (2)$$

For this application the cut-off frequency was set at $0.7Hz$ and the amplifier was configured with a gain of 2.02. This relatively low gain value was dictated by the limited voltage headroom of the INA116, which was operated with only a 5V supply (datasheet recommends 10V).

It is also worth noting that a similar 'bias-free' technique can also be applied successfully to rail-to-rail input/output operational amplifiers configured in unity gain by simply leaving the non-inverting input floating and AC coupling the output to the next stage. As long as DC measurements are not needed (as in EEG/ECG applications), the amplifier is guaranteed to operate somewhere inside the supply rails. We have successfully tested this with the LMC6081 and LMP7702 operational amplifiers (Fig. 5). The overall performance is comparable to the INA116 circuit. More detailed characterization of the design will be explored in a future paper.

To ensure that the electrode's gain is constant over a wide range of coupling distances, a small amount of positive

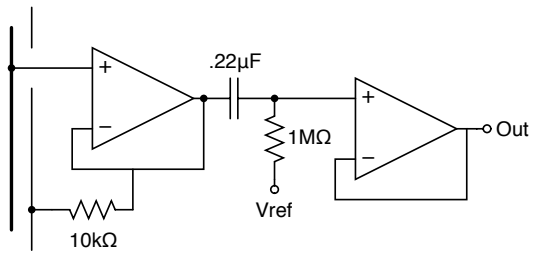

Fig. 5. Alternative analog front-end for the electrode using the LMP7702 operational amplifier.

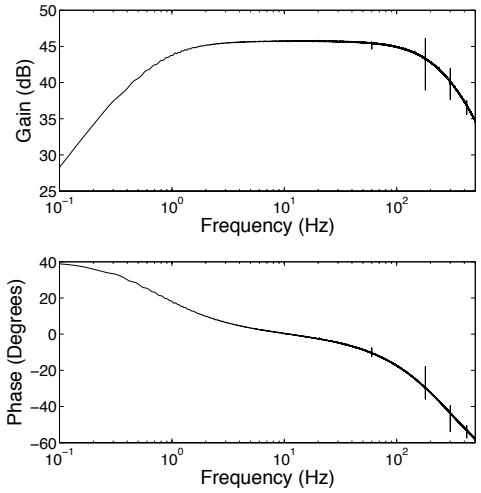

Fig. 6. Measured transfer function of the non-contact electrode.

feedback, adjusted by R_3, is applied back to the input through C_2. Each electrode is carefully calibrated at a test-bench by adjusting R_3 until the gain is constant for different coupling distances. In practice, however, the capacitance neutralization circuit is not needed since the system is wireless with a floating ground – no significant 50/60Hz mains interference is observed even with mismatched electrodes.

C. Differential Amplifier and ADC

The output of the INA116 is coupled to a differential gain amplifier through an additional high-pass filter with a cutoff of $.1Hz$ to remove the relatively high DC offset of the INA116. The LTC6078 micropower operational amplifier was chosen for it's excellent low noise and low offset characteristics. A simple non-inverting differential gain stage of $40.1dB$ was implemented by connecting the electrodes together through the node V_{cm}, which is carried in the daisy chain. This constructs what is essentially a multi-channel instrumentation amplifier to remove the common-mode noise while amplifying the local biopotential signal. A more detailed description of the circuit can be found in [9].

Figure 6 shows the full measured transfer function of the front-end and differential amplifier. A gain of $46dB$ and cutoff frequencies of $0.7Hz$ and $100Hz$ were obtained as expected.

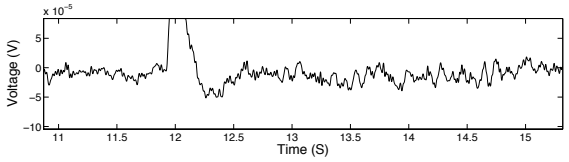

Fig. 8. Close-in plot of EEG trace from Fig. 7 showing the onset of alpha waves after the subject closed his eyes.

The total in-band input referred noise was measured to be $3.8\mu V$ RMS. At present, it appears that the noise pickup from external sources is as problematic, if not more so, as the intrinsic noise sources in the circuit, even with the active shield layer. This is not surprising due to the sensitivity of the ultra-high impedance input node. Future versions of the electrode will incorporate more comprehensive shielding strategies than a simple inner PCB plane.

D. Wireless Base Unit

The daisy chain of electrodes is terminated at one end to a simple wireless base unit which supplies the power and control signals. A simple, low power microprocessor (PIC24) bridges the serial data from the electrode's ADC to a standard commercial Bluetooth module (F2M03ALA). Bluetooth was utilized in this embodiment due to it's ease of use, high market penetration and compatibility. In this implementation, the serial port profile was utilized to rapidly develop a receiver application on a PC. However, a different wireless architecture can also easily be used for lower power consumption, depending on application.

Subject grounding is achieved with an actively driven ground connection. The common mode signal, V_{cm} is connected to an inverting amplifier with gain of -100 to provide an additional 40dB of CMRR for the system. The output of this amplifier is connected to the subject via a standard adhesive ECG electrode, and is the only physical contact to the user. In practice however, it was found that even a simple passive dry contact to the system ground is sufficient, since the wireless system is battery powered and floating close to the body, minimizing the effect of 50/60Hz line noise.

The entire system consumes approximately $300mW$, mostly dominated by the requirements of the PIC and bluetooth unit.

For the experiments below, a simple PC based application was written to acquire and store data from the telemetry for the body sensor network.

III. Physiological Data

Several measurements were taken with the wireless system to demonstrate the high signal quality obtained with the non-contact electrodes.

Figure 7 shows both a spectrogram and a time domain plot of a sample EEG recording with two electrodes in the FzA1 locations. The subject's eyes are open for the first half of the recording with eye blinks clearly visible. After the subject's eyes close, power near the 10Hz band can be observed showing the presence of alpha activity. A closer view of the EEG signal and alpha waves can be seen in Fig. 8.

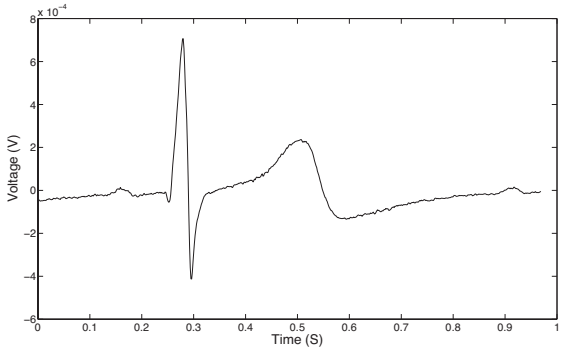

Fig. 9. Sample high-resolution ECG trace taken from the electrodes directly on top of the skin over the chest. The entire sequence of PQRST waves can be clearly seen and the signal is comparable to that obtained through adhesive contact sensors.

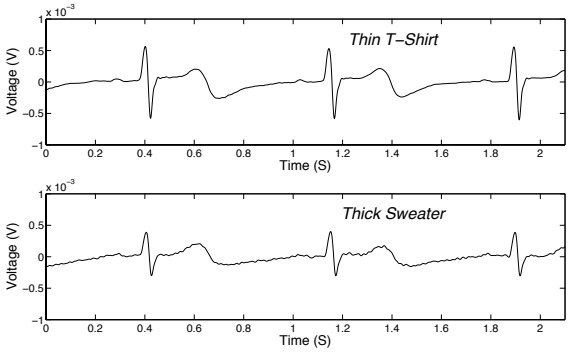

Fig. 10. ECG data on the chest through taken through a thin t-shirt and a thicker cotton sweater.

In addition, several experiments were carried out to test the performance of the electrodes for cardiac applications. Figure 9 shows the best case performance with the electrode pressed against the skin on the chest, with only the PCB soldermask acting as insulation. The entire PQRST complex can be clearly seen and the trace is comparable in quality to that obtained with a standard clinical adhesive ECG electrode.

As mentioned previously, one of the main advantages with non-contact electrodes is the ability to work through insulation such as fabric and clothing. Two traces are shown in Fig. 11 showing ECG data obtained on over the chest through a thin t-shirt and a thick cotton sweater. The signal generally remains clear through very thin insulating layers. Noise begins to be a problem with thicker insulation, obscuring smaller features such as the P-wave, but the signal quality is still more than sufficient for heart beat detection.

Finally, Figure 11 shows the data obtained from the sensors with a subject moving and jumping vigorously with the electrodes in pressed tightly against the body. The trace remains stable over the 100 second recording even in the presence of motion.

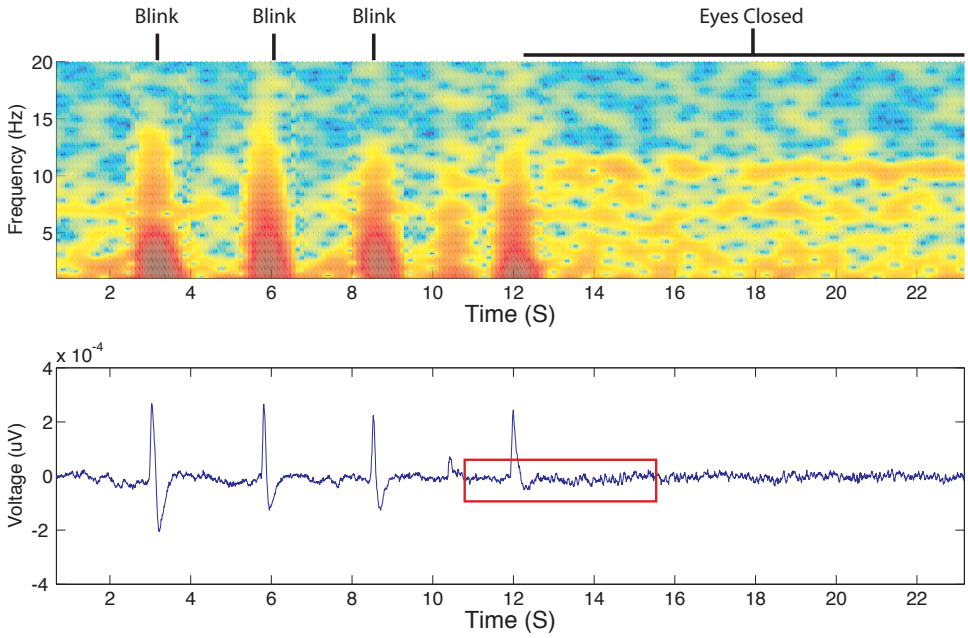

Fig. 7. Spectrogram and time domain plot of EEG data. Power in the alpha band can be observed after the subject's eyes close. A close up of the EEG signal outlined in red can be seen in Fig. 8

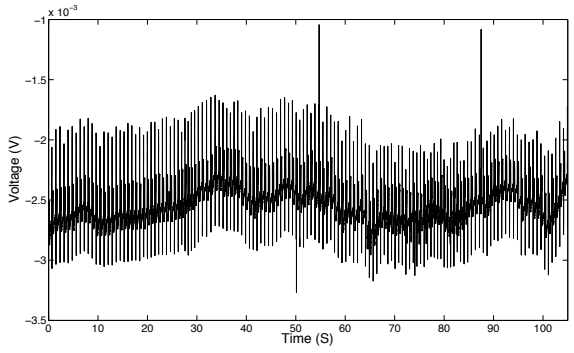

Fig. 11. Plot of ECG data taken on the chest over a 100 second period showing a stable trace even with an actively moving subject.

IV. Conclusion

We present a wireless body sensor network for high quality EEG/ECG recordings utilizing non-contact electrodes. The full schematics for building the simple, low noise capacitive electrode are presented. Future work will focus on miniaturizing and better packaging the electrode as well as reducing the power consumption of the digital and wireless transmitter components.

References

[1] T.J. Sullivan, S.R. Deiss, T.-P. Jung, and G. Cauwenberghs. A brain-machine interface using dry-contact, low-noise EEG sensors. *Proc. IEEE Int. Symp. Circuits and Systems (ISCAS'2008)*, May 2008.

[2] E.S. Valchinov and N.E. Pallikarakis. An active electrode for biopotential recording from small localized biosources. *Biomedical engineering Online*, 3, July 2004.

[3] A. Lopez and P. C. Richardson. Capacitive electrocardiographic and bioelectric electrodes. *IEEE Transactions on Biomedical Engineering*, 16:299–300, 1969.

[4] T.J. Sullivan, S.R. Deiss, and G. Cauwenberghs. A low-noise, non-contact EEG/ECG sensor. *Proc. IEEE Biomedical Circuits and Systems Conf. (BioCAS'2007)*, November 2007.

[5] C.J. Harland, T.D. Clark, and R.J. Prance. Electric potential probes - new directions in the remote sensing of the human body. *Measurement Science and Technology*, 2:163–169, February 2002.

[6] R. Matthews, N. J. McDonald, P Hervieux I. Fridman, and T. Nielsen. The invisible electrode zero prep time, ultra low capacitive sensing. *Proceedings of the 11th International Conference on Human-Computer Interaction*, July 2005.

[7] P. Park, P.H. Chou, Y. Bai, R. Matthews, and A. Hibbs. An ultra-wearable, wireless, low power ECG monitoring system. *Proc. IEEE International Conference on Complex Medical Engineering*, pages 241–244, Nov 2006.

[8] S.R. Deiss Y.M. Chi and Gert Cauwenberghs. Non-contact low power eeg/ecg electrode for high density wearable biopotential sensor networks. *IEEE BSN 2009*, June 2009.

[9] Y.M. Chi and Gert Cauwenberghs. Micropower non-contact eeg electrode with active common-mode noise suppression and input capacitance cancellation. *IEEE Engineering in Medicine and Biology*, September 2009.

[10] R.J. Prance, T.D. Clark, H. Prance, and A. Clippingdale. Non-contact VLSI imaging using a scanning electric potential microscope. *Measurement Science and Technology*, 8:1229–1235, August 1998.

[11] K Melhorn M Oehler, V Ling and M Schilling. A multichannel portable ecg system with capacitive sensors. *Physiological Measurement*, 29:783–793, July 2009.

[12] T. Maruyama, M. Makikawa, N. Shiozawa, and Y. Fujiwara. ECG measurement using capacitive coupling electrodes for man-machine emotional communication. *Proc. IEEE International Conference on Complex Medical Engineering*, pages 378–383, May 2007.

[13] P. Park, P.H. Chou, Y. Bai, R. Matthews, and A. Hibbs. A barium-titanate-ceramics capacitive-type EEG electrode. *IEEE Transactions on Biomedical Engineering*, pages 299–300, July 1973.

[14] A. Aleksandrowicz and S. Leonhardt. Wireless and non-contact ECG measurement system– the Aachen SmartChair. *ActaPolytechnica*, 2:68–71, June 2007.